

Cite this: *CrystEngComm*, 2012, 14, 6744–6749

www.rsc.org/crystengcomm

PAPER

## Polymorphism in co-crystals: a metastable form of the ionic co-crystal 2 HBz·1 NaBz crystallised by flash evaporation†

Christian Butterhof,<sup>a</sup> Kilian Bärwinkel,<sup>b</sup> Jürgen Senker<sup>b</sup> and Josef Breu<sup>\*a</sup>

Received 14th April 2012, Accepted 16th July 2012

DOI: 10.1039/c2ce25562f

While polymorphism is a wide spread phenomenon, the number of reported polymorphic co-crystals is still very limited. Here we report the synthesis and structural characterisation of such a rare case of polymorphism with a co-crystal of benzoic acid (HBz) and sodium benzoate (NaBz). Flash evaporation yielded a new polymorph of this ionic co-crystal with a stoichiometry of 2 HBz·1 NaBz. The thermodynamic relationship between the known and the new polymorph was determined to be of enantiotropic nature. At room temperature, this new form B is metastable. While the known form A is composed of one dimensional tapes, form B is built from infinite rods. The coordination sphere of sodium, however, in both forms is octahedral and the packing around it is dense.

### Introduction

According to McCrone's definition, polymorphism is the ability of a solid material to be crystallised in at least two crystalline forms.<sup>1</sup> Polymorphism has gained great interest in the last decades, mainly for two reasons.<sup>2–6</sup> On one hand different polymorphs exhibit different physicochemical properties like melting point, moisture sorption tendency, chemical stability, compressibility, processability, and solubility.<sup>7,8</sup> On the other hand different polymorphs of the same material can often be protected by patent and therefore are of crucial economic importance.<sup>9</sup> The origin of polymorphism can be classified into two categories. Firstly identical molecular moieties may be packed into different periodic crystal structures. Secondly molecular moieties with rotational degrees of freedom may adopt different conformations in solution that lead to distinct packings in the crystal. The first is called packing polymorphism and the second conformational polymorphism.<sup>10</sup> In most polymorphic systems a mixture of both forms occurs concomitantly.

For similar reasons as polymorphs, recently co-crystals have received increasing attention in the field of crystal engineering.<sup>11–13</sup> These are built up by at least two components which are solid under ambient conditions. Nevertheless, co-crystallisation influences the same before mentioned properties, just like with different polymorphs.<sup>14,15</sup> Very few examples of ionic co-crystals or hybrid salt co-crystals, where a metal halide is co-crystallized together with an organic co-crystal former, have been reported.<sup>16–18</sup>

Because of the economical importance of both polymorphs and co-crystals, the number of characterised polymorphs (~2050) and co-crystals (~3650) increases steadily. Interestingly, the number of reported polymorphic co-crystals (~50) is still minute.<sup>19</sup> Here we report such a rare case of polymorphism with co-crystals.

The relative stability of two polymorphs depends on the difference in Gibbs free energy. The thermodynamically stable form at fixed temperature and pressure has the lowest Gibbs free energy, while others are metastable in respect to this. Especially in the pharmaceutical industry the metastable form can often be favourable, because of its higher solubility and therefore higher bioavailability. Despite this, intentional and systematic crystallisation of metastable forms remains very difficult because nucleation is not well understood. The best working rule of thumb is summarised in Ostwald's step rule suggesting that high supersaturations might induce crystallisation of metastable polymorphs. Reproduction of known metastable polymorphs is no less complicated than detection of new polymorphs because frequently crucial crystallisation parameters were not recognised nor documented.<sup>20</sup> Moreover, crystallisation of phase-pure metastable compounds is frequently hampered by secondary nucleation of more stable polymorphs followed by (partial) solution-mediated transformation. For instance, in this line, all metastable forms of the first molecular polymorphic system mentioned in the literature, benzamide, are obtained as mixtures, and as many as three concomitantly crystallising polymorphs have been reported.<sup>21–24</sup>

Following Ostwald's step rule, fast evaporation has been extensively used to create high levels of supersaturation to form metastable polymorphs. For instance, Bag *et al.* described the use of a rotary evaporator, while Williams *et al.* and Breu *et al.* quickly evaporated warm solutions by a flow of nitrogen.<sup>25–28</sup> Since the method used here provides even higher evaporation rates and thus higher supersaturations, we refer to it as flash evaporation (details experimental section).

<sup>a</sup>Inorganic Chemistry I, University of Bayreuth, Universitätsstraße 30, 95440 Bayreuth, Germany. E-mail: josef.breu@uni-bayreuth.de;

Fax: +49 921 55-2788; Tel: +49 921 55-2530

<sup>b</sup>Inorganic Chemistry III, University of Bayreuth, Universitätsstraße 30, 95440 Bayreuth, Germany

† CCDC 875039 and 875040. For crystallographic data in CIF or other electronic format see DOI: 10.1039/c2ce25562f

Recently we investigated the influence of stoichiometry for the co-crystallisation of benzoic acid (HBz) with sodium benzoate (NaBz).<sup>29</sup> In the course of these investigations, we now obtained a new metastable form of the ionic co-crystal 2 HBz·1 NaBz.

## Results and discussion

The metastable form B of the co-crystal 2 HBz·1 NaBz was obtained according to Ostwald's rule by generating high supersaturations and applying flash evaporation of the solvent.<sup>25</sup> Very high evaporation rates of a solution containing the two co-crystal components may be achieved using a solvent with low boiling point and relatively high vapour pressure. In that respect, methanol is a good choice having a boiling point of  $\sim 64.7$  °C and a vapour pressure of 144.55 kPa at 75 °C (calculated with the Antoine constants of methanol).<sup>30</sup> Form A of 2 HBz·1 NaBz was obtained by slow evaporation of an ethanol–water (4 : 1/ v : v) solution over three days. Contrary to this, flash evaporation of a boiling solution in pure methanol on a hot plate yielded crystals which already differ significantly in crystal morphology from the known co-crystal of form A (Fig. 1). For details of the crystallisation see experimental section. Despite the rough and fast crystallisation we obtained single crystals of sufficient quality for structure determination. At room temperature, crystals of form B deteriorated within 24 h hours. Even at  $-100$  °C the total time available for data collection was limited by the stability of form B. Although the best data set available was relatively weak due to the limited size and stability, we were nevertheless able to determine the crystal structure of form B of the co-crystal 2 HBz·1 NaBz which will be discussed and compared to form A in the first part of this publication. In the second part it will be shown that this new polymorph is metastable at room temperature compared to the known form A and that the phase transition is of the enantiotropic type.

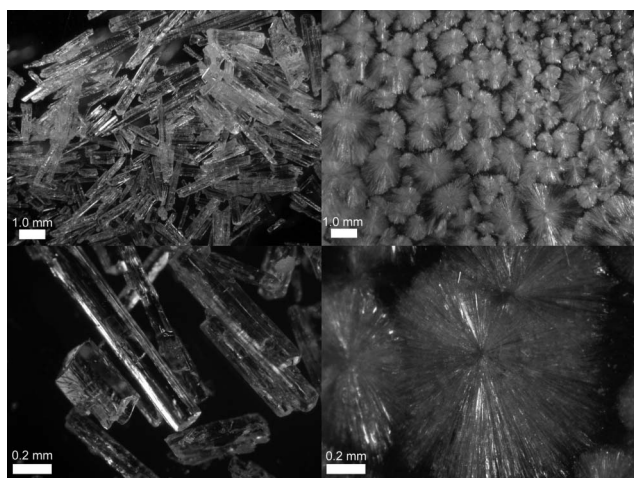


**Fig. 1** Light microscopy images of the two polymorphic forms of the co-crystal 2 HBz·1 NaBz. Form A, the thermodynamically stable form at room temperature is shown on the left, form B on the right side. Crystals of form B grow in a rose-like fashion, while form A crystallises in large prisms.

## The crystal structure of form B of the co-crystal 2 HBz·1 NaBz

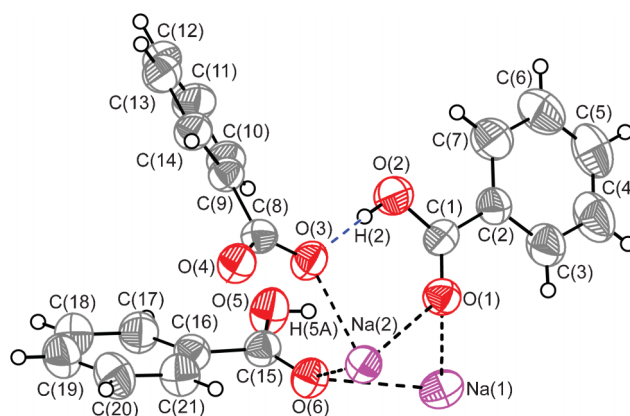
Crystal structure solution and refinement turned out to be straightforward, although in the light of the limited stability and crystal sizes available of form B, optimum data collection was a compromise between data completeness and signal to noise ratio.

Table 1 shows the crystallographic data for form B of the 2 HBz·1 NaBz co-crystal, while the asymmetric unit is shown in Fig. 2. The packing and its construction from building units is shown in Fig. 3. While form A is built from one-dimensional tapes of dimers, the crystal structure of form B is composed of rods (Fig. 3a). Each rod is surrounded by six neighbouring rods in an approximately hexagonal array. Much similar in both forms, between the tapes in form A and the rods in form B, van der Waals forces and  $\pi$ - $\pi$ -stacking motifs are the main interaction forces. As clearly evident in the projection along the *a*-axis, the molecular packing in form B contains classical

**Table 1** Crystallographic data for the co-crystal 2 HBz·1 NaBz

	Form B (173 K)	Form A (173 K)
Formula	C <sub>21</sub> H <sub>17</sub> NaO <sub>6</sub>	C <sub>21</sub> H <sub>17</sub> NaO <sub>6</sub>
Formula weight	388.34	388.34
<i>T</i> /K	173(2)	173(2)
Crystal system	Triclinic	Monoclinic
Space group	<i>P</i> $\bar{1}$	<i>P</i> 2 <sub>1</sub> / <i>c</i>
<i>a</i> /Å	6.8912(14)	5.8402(12)
<i>b</i> /Å	12.082(2)	14.499(3)
<i>c</i> /Å	13.372(3)	22.136(4)
$\alpha$ (°)	109.97(3)	90
$\beta$ (°)	100.51(3)	97.18(3)
$\gamma$ (°)	103.88(3)	90
<i>V</i> Å <sup>3</sup>	972.3(3)	1859.7(6)
<i>Z</i>	2	4
<i>D</i> <sub>c</sub> /g cm <sup>-3</sup>	1.326	1.387
$\mu$ /mm <sup>-1</sup>	0.116	0.121
<i>R</i> <sub>int</sub>	0.0896	0.109
Refln (all/ind)	3576/1209	3466/2140
<i>R</i> <sub>1</sub> / <i>wR</i> <sub>2</sub> (obsd data: $F^2 > 2\sigma(F^2)$ ) <sup>a</sup>	0.0461/0.0920	0.0411/0.0983
<i>R</i> <sub>1</sub> / <i>wR</i> <sub>2</sub> (all data) <sup>a</sup>	0.1309/0.1643	0.0723/0.1173
Largest residual/e Å <sup>-3</sup>	0.235	0.224

<sup>a</sup>  $R_1 = (||F_o| - |F_c||)/\Sigma|F_o|$ ;  $wR_2 = [\Sigma w(|F_o| - |F_c|)^2]/\Sigma w(F_o)^2]^{1/2}$ .



**Fig. 2** ORTEP plot and the crystallographic numbering scheme of the asymmetric unit for form B of the co-crystal 2 HBz·1 NaBz. Displacement ellipsoids are drawn at the 50% probability level. Please note that both sodium cations reside on special positions (Wyckoff sites 1d and 1a for Na(1) and Na(2), respectively).

four-fold phenyl embraces<sup>31</sup> at the centre of the unit cell, around the inversion centre at 0, 0.5, 0.5. In addition, there are oblique edge-to-face (T-shaped) interactions between pairs of phenyl groups across a point near 0, 0.25, 0.5. The  $\pi$ - $\pi$  interaction distances between adjacent phenyl rings (Fig. 2c), in form B are 4.04(5) Å (C(9)–C(14)) and 4.55(7) Å (C(16)–C(21)), respectively. These are much longer compared to distances in form A (3.83(8) Å and 3.92(2) Å). A side view on the rod shows that Na(1) and Na(2) reside, as expected, in a strongly distorted octahedral coordination (see Fig. 3b, Fig. 4 and Fig. 5). A space filling

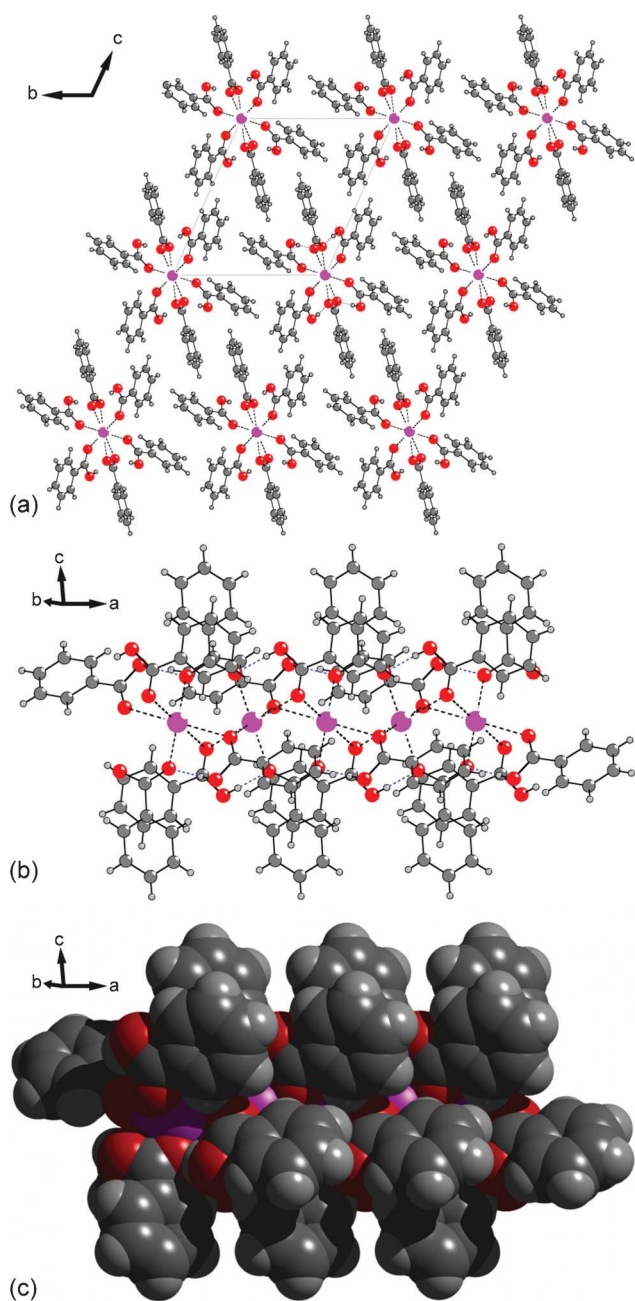


**Fig. 3** Molecular packing of form B of the co-crystal 2 HBz:1 NaBz of HBz with NaBz. (a) Approximately hexagonal packing of rods running along the *a*-axis. (b) Side view on one of these rods. Coordination bonds are dashed in black and hydrogen bonds are dashed in blue. (c) Space filling model of the rod.

model (Fig. 3c) highlights that the packing in the rod is dense, similar to form A.

In form A, two octahedra are connected *via* a shared edge and then these dimers form infinite tapes running into the plane of the paper *via* bridging carboxylic/carboxylate groups (for details see ref. 29 and (Fig. 4a). In form B, however, each octahedron shares two edges with two adjacent octahedra resulting in infinite rods running from left to right (Fig. 4b and Fig. 5). Tapes of form A and rods of form B are compared in Fig. 5. The different Na–O distances in form A and form B are shown in Fig. 4.

In form B only carbonyl oxygens of carboxylic acid groups (HBz), displayed in orange (O(1), O(6)), are involved in all shared edges. All HBz molecules therefore act as monodentate ligands. Contrary to this, the carboxylate groups (NaBz), displayed in red (O(3), O(4)), act as bidentate ligands occupying apical positions of adjacent octahedra (Fig. 5) which causes strong tilting of the neighbouring octahedra. The pending, free hydroxyl oxygens (O(2), O(5)) reinforce the chain by forming H-bonds (Table 2) to adjacent NaBz (Fig. 5).

IR-spectra of both polymorphic forms are compared in Fig. 6. In line with the quite different intermolecular arrangements and packing modes of both forms, the spectra differ significantly.

#### Packing polymorphism versus conformational polymorphism.

HBz and NaBz are quite simple molecules having only one torsional degree of freedom, suggesting that polymorphism is mostly related to packing and less to torsional degrees of freedom. As discussed, the packing motifs of form A and B differ significantly. A closer look, however, reveals that the torsion angles also are quite different. Strong variations are observed between different moieties within a given form but also between the two forms (Table 3). Therefore, the intramolecular energies will have some contributions to the lattice energies and even with this simple molecule a mixture between packing and conformational polymorphism is found.<sup>10</sup>

#### Thermodynamic relation between form A and B

To elucidate the thermodynamic relation between the two polymorphic forms, we carried out several additional experiments and performed theoretical calculations.

**DFT calculations.** In order to determine the energetically more stable form we carried out geometry optimisations for both forms applying density functional theory with semi-empirical dispersion correction (DFT-D).<sup>32,33</sup> DFT-D level was used because it is well known that at the DFT level of theory dispersion energies are underestimated and the ranking of many organic crystals was found to be in error.<sup>34</sup> The crystal structures as determined by single crystal refinements using data collected at 173 K were optimised applying the Broyden–Fletcher–Goldfarb–Shannon algorithm.<sup>35</sup> The lattice parameters were included into the optimisation and the space group symmetry was taken as *P1*. The total energies of form A and B as obtained for the DFT-D relaxed geometries are summarised in Table 4.

The calculation implies that at 0 K form B is metastable by as little as 0.08 kJ mol<sup>−1</sup>. Considering that entropy effects are neglected, the ranking of the two forms cannot be determined reliably based on DFT-D calculations.

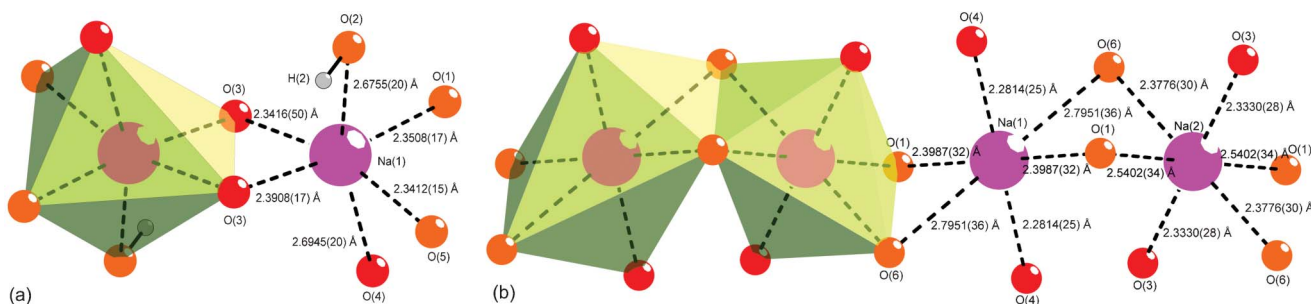


**Fig. 4** Coordination spheres of sodium in form A and B of the co-crystal 2 HBz-1 NaBz. Oxygen atoms belonging to carboxylic groups (HBz) are in orange, while oxygen atoms belonging to carboxylate groups (NaBz) are in red. The Na–O distances show the strongly distorted octahedral coordination in both forms (both measured at 173 K). The distances in form B are longer compared to the thermodynamically stable form A at room temperature.

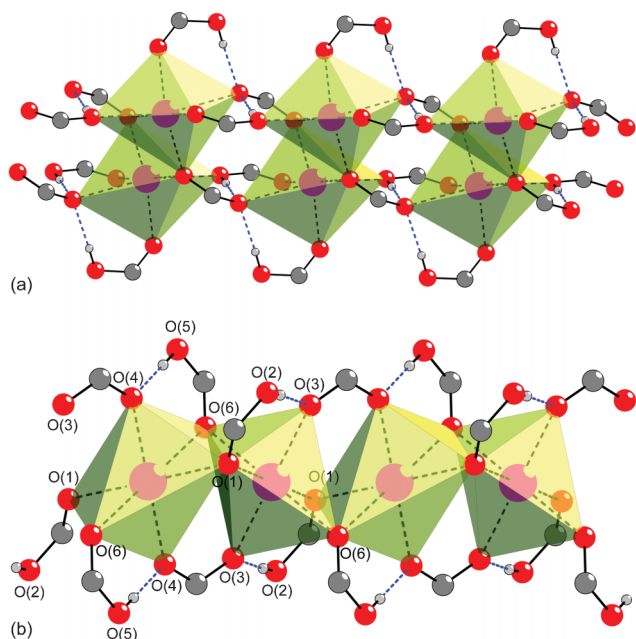


**Fig. 5** Comparison of the connection of octahedra in form A and B of the co-crystal 2 HBz-1 NaBz. For clarity reasons, phenyl rings of HBz and NaBz are not shown. Hydrogen bonds are dashed in blue. (a) One-dimensional tape of edge-sharing octahedra in form A. (b) Infinite rods of edge-sharing octahedra in form B.

**Table 2** Summary of intermolecular interactions (D–H···A; Å, °) operating in the crystal structure of form B of the co-crystal 2 HBz-1 NaBz

D	H	A	H···A/Å	D···A/Å	∠(DHA)/°	Symmetry operation
O(2)	H(2)	O(3)	1.73	2.551(4)	174.7	$x, y, z$
O(5)	H(5)	O(4)	1.74	2.558(5)	178.7	$x + 1, y, z$

**Solution mediated transformation.** To experimentally determine the thermodynamic ranking at room temperature, we filled a 1 : 1 ratio of both forms into a capillary, which was then soaked with ethanol, sealed, and mounted on a powder diffractometer equipped with a fast and high resolution detector. Within 40 min form B is completely transformed into form A (Fig. 7) at room temperature which unequivocally proves form B to be metastable at this temperature. This ranking is in agreement with the density rule,

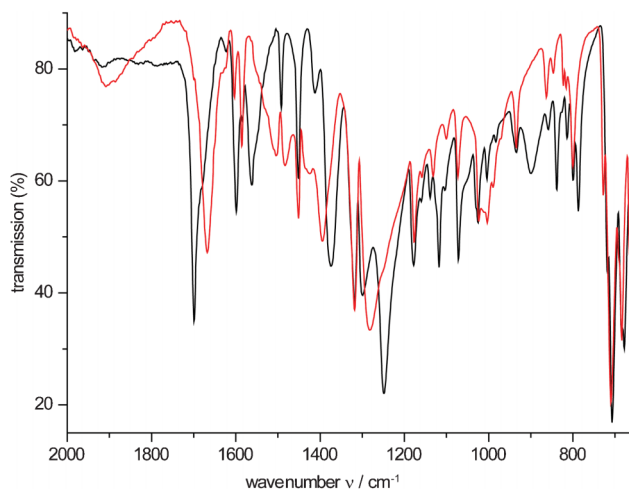


**Fig. 6** IR spectroscopy of the two polymorphs of the co-crystal 2 HBz-1 NaBz. The black trace corresponds to form A and the red trace to the metastable form B. Because of the different packing the differences are obvious.

**Table 3** Comparison of the torsional angles (°) in form A and B

	Form A	Form B
HBz 1	6.18 (O1–C1–C2–C7)	0.45 (O2–C1–C2–C7)
	8.30 (O2–C1–C2–C3)	2.19 (O1–C1–C2–C3)
HBz 2	2.54 (O6–C15–C16–C17)	14.67 (O5–C15–C16–C17)
	6.53 (O5–C15–C16–C21)	18.13 (O6–C15–C16–C21)
Bz <sup>−</sup>	11.83 (O3–C8–C9–C14)	27.52 (O4–C8–C9–C14)
	12.14 (O4–C8–C9–C10)	29.40 (O3–C8–C9–C10)

since both experimental and theoretical densities (DFT-D) of form A are higher than the densities of form B (A: 1.387 g cm<sup>−3</sup> (173 K) and 1.450 g cm<sup>−3</sup> (0 K, DFT-D); B: 1.326 g cm<sup>−3</sup> (173 K) and 1.386 g cm<sup>−3</sup> (0 K, DFT-D).

While the solution-mediated transformation is also in line with the total energies obtained in the DFT-D calculations, it delivers, however, no information on the nature of the transformation (enantiotropic or monotropic).

Burger introduced several rules to determine the thermodynamic relation in polymorphs.<sup>36</sup> One of the most important rules, the heat-of-fusion rule could not be applied because reliable DSC measurements are not feasible. Because both

**Table 4** Summary of the CASTEP geometry optimisation. The deviation of the optimised structure parameters as compared to the experimentally determined crystal structures at 173 K are given in brackets

Form	Lattice parameters	$\Delta E$ (kJ mol <sup>-1</sup> )	
A	$a/\text{\AA}$	5.770 (-1.21%)	0
	$b/\text{\AA}$	14.331 (-1.16%)	
	$c/\text{\AA}$	21.621 (-2.33%)	
	$\alpha$ (°)	90.00 (0.0%)	
	$\beta$ (°)	95.85 (-1.37%)	
	$\gamma$ (°)	90.00 (0.0%)	
	$V/\text{\AA}^3$	1778.5	
B	$a/\text{\AA}$	6.912 (0.30%)	+0.08
	$b/\text{\AA}$	11.624 (-3.79%)	
	$c/\text{\AA}$	13.169 (-1.52%)	
	$\alpha$ (°)	107.80 (-1.98%)	
	$\beta$ (°)	99.98 (-0.53%)	
	$\gamma$ (°)	105.82 (1.87%)	
	$V/\text{\AA}^3$	930.5	

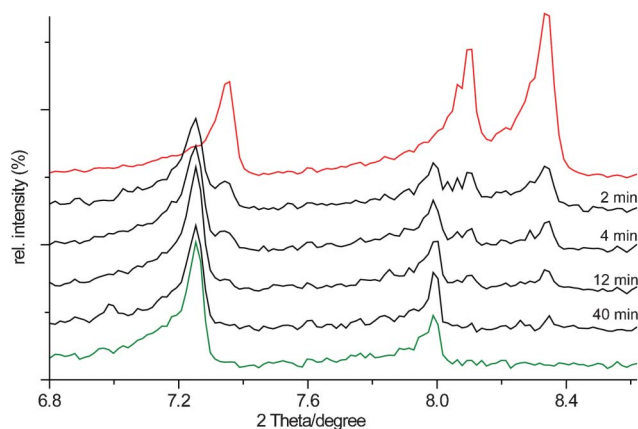


**Fig. 7** Solution mediated transformation of a mixture of form A and B at room temperature (slurry with ethanol). The red trace corresponds to pure form B and the green trace to pure form A. The black traces correspond to the slurry of the mixture of form A and B measured after different time intervals.

polymorphs readily lose benzoic acid upon heating we refrained from determining melting enthalpies.

Flammersheim referred to a “high-temperature” modification in his work.<sup>37</sup> He claimed that 2 HBz·1 NaBz of form A

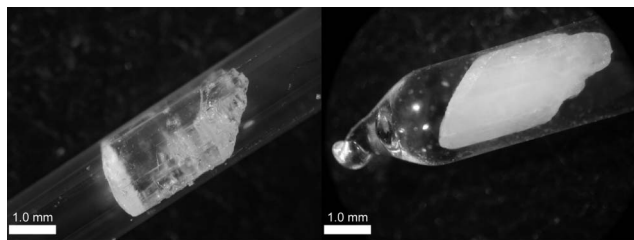


**Fig. 8** Light microscopy images of the enantiotropic phase transition of the co-crystal 2 HBz·1 NaBz. On the left side a large single-crystal of form A, which is the thermodynamically stable form at room temperature, was put into a capillary. The capillary was sealed and heated to 110 °C for one day. After heating the large single crystal of form A transformed into many small micro-crystallites. These can be assigned as crystallites of form B by powder diffraction.

undergoes a phase transition into a “high-temperature” form upon heating the crystals to 120 °C. But he also mentioned severe problems caused by sublimation.

For this reason we attempted a solid–solid phase transition of a large crystal of form A in a gas-tight sealed quartz-capillary. The capillary was annealed for one day at 110 °C. Fig. 8 shows light microscopy images of a single crystal before and after the annealing. PXRD of the annealed crystal indicates a complete transformation of form A into form B. As suggested by the opaqueness of the annealed crystal, the transformation did not occur single crystal to single crystal but a microcrystalline powder was obtained. Phase purity was verified by performing a Pawley refinement using TOPAS<sup>38</sup> of the unit cell parameters (Fig. 9). Thus, the thermodynamic relation of form A and B can be assigned as enantiotropic. Comparing a list of d-values published by Flammersheim for the “high-temperature” modification (Table 5), this modification appears to be identical to form B.

## Experimental

NaBz (purity  $\geq 99.0\%$ ) and HBz (purity  $>99.5\%$ ) were purchased from AppliChem. Methanol was sourced from Sigma-Aldrich. All chemicals and solvents were used without further purification.

PXRD traces were recorded using a STOE STADI P (CuK<sub>α1</sub> radiation, transmission geometry) diffractometer equipped with a DECTRIS Mythen 1 K silicon strip detector. The samples were filled in capillaries (diameter 0.5 mm and 2.0 mm). Single-crystal X-ray diffraction data were collected using a STOE IPDS I instrument (293 K, MoK<sub>α</sub> radiation). Selected crystallographic data are listed in Table 1. The crystal structure was solved and refined using SHELXTL 5.1 (Bruker AXS). All figures were drawn with the DIAMOND programme. IR spectroscopy was performed

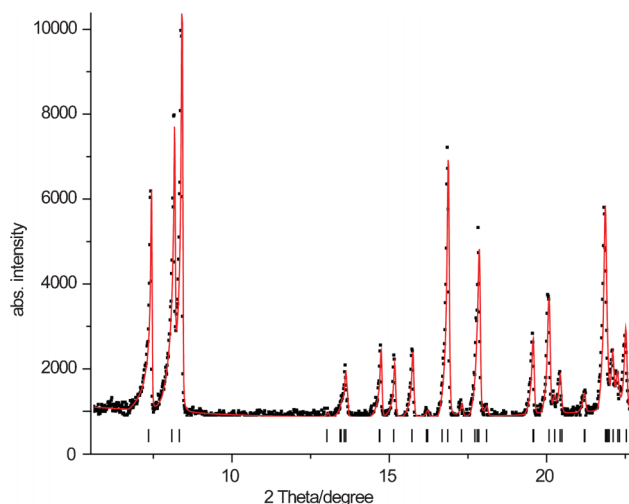


**Fig. 9** Pawley refinement (applying TOPAS<sup>38</sup>) of unit cell parameters of form B of the co-crystal 2 HBz·1 NaBz obtained by annealing a single crystal of form A at 110 °C. All reflections can be indexed by the unit cell parameters showing phase purity and complete conversion of form A into B ( $R_{wp} = 6.248$ ; zero point =  $-0.026(4)^\circ$  2 Theta;  $a = 6.9065(5) \text{\AA}$ ;  $b = 12.2522(7) \text{\AA}$ ;  $c = 13.4431(7) \text{\AA}$ ;  $\alpha = 111.346(5)^\circ$ ;  $\beta = 101.121(5)^\circ$ ;  $\gamma = 101.953(6)^\circ$ )

**Table 5** Comparison of selected d-values reported by Flammersheim for the “high-temperature” phase of the co-crystal 2 HBz·1 NaBz and the metastable form B described in this work. The agreement shows that both are likely to be identical

Flammersheim <sup>37</sup>	This work
12.06	11.966
10.92	10.874
10.59	10.557
5.62	5.596
5.46	5.437
5.24	5.226
4.94	4.948
4.51	4.498

on a PerkinElmer Spectrum 100 FT-IR spectrometer working with the UATR (universal attenuated total reflectance) technique.

The DFT-D calculations were carried out using the CASTEP code.<sup>39</sup> The generalised-gradient approximation (GGA) with the Perdew–Burke–Ernzerhof (PBE) functional was used.<sup>40</sup> A plane-wave basis set with an energy cutoff of 900 eV was applied and the core electrons were represented by pseudopotentials. For the geometry optimisation the convergence tolerances of energy, maximum force, maximum displacement were  $2.0 \times 10^{-5}$  eV per atom,  $5.0 \times 10^{-2}$  eV Å<sup>-1</sup> and  $1.0 \times 10^{-3}$  Å, respectively. The allowed stress tolerance was 0.1 GPa.

### Flash evaporation crystallisation

Single crystals were obtained from a solution of 2.442 g (20.00 mmol) HBz and 1.441 g (10.00 mmol) NaBz in 15 ml methanol. This mixture was heated to 65 °C, until all starting material was dissolved. Afterwards ~3 ml of the hot solution were spread on a heated (~75 °C) crystallising dish (Ø ~ 15 cm). Within seconds methanol evaporates and colourless crystals can be observed (see Fig. 1).

### Conclusions

The thermodynamic relationship between the two polymorphs of the ionic co-crystal 2 HBz·1 NaBz was determined to be of enantiotropic nature with a transformation temperature below 110 °C. At room temperature, form B is metastable. While form A is composed of one-dimensional tapes, form B is built from infinite rods. The coordination sphere of sodium, however, in both co-crystals is octahedral and the packing around it is dense.

### Acknowledgements

We thank the Deutsche Forschungsgemeinschaft (SPP 1415), for financial support. The authors thank Karl Kempf and Prof. Dr Rainer Schobert for measurement of the IR spectra. We would like to thank an anonymous referee for valuable comments.

### References

- 1 J. Haleblia and W. McCrone, *J. Pharm. Sci.*, 1969, **58**, 911–929.
- 2 D. Braga, F. Grepioni and L. Maini, *Chem. Commun.*, 2010, **46**, 6232–6242.

- 3 H. G. Brittain, *J. Pharm. Sci.*, 2008, **97**, 3611–3636.
- 4 *Polymorphism in the Pharmaceutical Industry*, ed. R. Hilfiker, Wiley-VCH Verlag, Weinheim, Germany, 2006.
- 5 K. Sato, *Chem. Eng. Sci.*, 2001, **56**, 2255–2265.
- 6 *Pharmaceutical Salts and Co-crystals*, ed. J. Wouters and L. Quéré, Royal Society of Chemistry, 2011.
- 7 S. R. Chemburkar, J. Bauer, K. Deming, H. Spiwek, K. Patel, J. Morris, R. Henry, S. Spanton, W. Dziki, W. Porter, J. Quick, P. Bauer, J. Donaubaue, B. A. Narayanan, M. Soldani, D. Riley and K. McFarland, *Org. Process Res. Dev.*, 2000, **4**, 413–417.
- 8 Y. Kobayashi, S. Ito, S. Itai and K. Yamamoto, *Int. J. Pharm.*, 2000, **193**, 137–146.
- 9 J. O. Henck, U. J. Griesser and A. Burger, *Pharm. Ind.*, 1997, **59**, 165–169.
- 10 S. R. Vippagunta, H. G. Brittain and D. J. W. Grant, *Adv. Drug Delivery Rev.*, 2001, **48**, 3–26.
- 11 C. B. Aakeröy and D. J. Salmon, *CrystEngComm*, 2005, **7**, 439–448.
- 12 O. Almarsson and M. J. Zaworotko, *Chem. Commun.*, 2004, 1889–1896.
- 13 P. Vishweshwar, J. A. McMahon, J. A. Bis and M. J. Zaworotko, *J. Pharm. Sci.*, 2006, **95**, 499–516.
- 14 N. J. Babu and A. Nangia, *Cryst. Growth Des.*, 2011, **11**, 2662–2679.
- 15 N. Schultheiss and A. Newman, *Cryst. Growth Des.*, 2009, **9**, 2950–2967.
- 16 D. Braga, F. Grepioni, L. Maini, S. Prosperi, R. Gobetto and M. R. Chierotti, *Chem. Commun.*, 2010, **46**, 7715–7717.
- 17 D. Braga, F. Grepioni, G. I. Lampronti, L. Maini and A. Turrina, *Cryst. Growth Des.*, 2011, **11**, 5621–5627.
- 18 L. Leclercq, I. Suisse, G. Nowogrocki and F. Agbossou-Niedercorn, *J. Mol. Struct.*, 2008, **892**, 433–437.
- 19 S. Aitipamula, P. S. Chow and R. B. H. Tan, *Cryst. Growth Des.*, 2010, **10**, 2229–2238.
- 20 J. Bernstein, R. J. Davey and J. O. Henck, *Angew. Chem., Int. Ed.*, 1999, **38**, 3440–3461.
- 21 F. Wöhler and J. von Liebig, *Ann. Pharm.*, 1832, **3**, 249–282.
- 22 W. I. F. David, K. Shankland, C. R. Pulham, N. Blagden, R. J. Davey and M. Song, *Angew. Chem., Int. Ed.*, 2005, **44**, 7032–7035.
- 23 J. Thun, L. Seyfarth, C. Butterhof, J. Senker, R. E. Dinnebier and J. Breu, *Cryst. Growth Des.*, 2009, **9**, 2435–2441.
- 24 J. Thun, L. Seyfarth, J. Senker, R. E. Dinnebier and J. Breu, *Angew. Chem., Int. Ed.*, 2007, **46**, 6729–6731.
- 25 P. P. Bag, M. Patni and C. M. Reddy, *CrystEngComm*, 2011, **13**, 5650–5652.
- 26 P. P. Bag and C. M. Reddy, *Cryst. Growth Des.*, 2012, **12**, 2740–2743.
- 27 J. Breu, W. Seidl, D. Huttner and F. Kraus, *Chem.–Eur. J.*, 2002, **8**, 4454–4460.
- 28 P. A. Williams, G. E. Hughes, G. K. Lim, B. M. Kariuki and K. D. M. Harris, *Cryst. Growth Des.*, 2012, **12**, 3104–3113.
- 29 C. Butterhof, W. Milius and J. Breu, *CrystEngComm*, 2012, **14**, 3945–3950.
- 30 *Numerical Data and Functional Relationships in Science and Technology - Vapor Pressure of Chemicals*, ed. J. Dykyj, J. Svoboda, R. C. Wilhoit, M. Frenkel and K. R. Hall, Springer, Berlin Heidelberg, Germany, 2000.
- 31 I. Dance and M. Scudder, *CrystEngComm*, 2009, **11**, 2233–2247.
- 32 E. R. McNellis, J. Meyer and K. Reuter, *Phys. Rev. B*, 2009, **80**.
- 33 A. Tkatchenko and M. Scheffler, *Phys. Rev. Lett.*, 2009, **102**.
- 34 B. Civalieri, C. M. Zicovich-Wilson, L. Valenzano and P. Ugliengo, *CrystEngComm*, 2008, **10**, 405–410.
- 35 B. G. Frommer, M. Cote, S. G. Louie and M. L. Cohen, *J. Comput. Phys.*, 1997, **131**, 233–240.
- 36 A. Burger and R. Ramberger, *Microchim. Acta*, 1979, **72**, 259–271.
- 37 H. J. Flammersheim, *Krist. Tech.*, 1974, **9**, 299–311.
- 38 *TOPAS Academic Technical Reference, Version 4.1*, A. A. Coelho, Bruker AXS GmbH, Karlsruhe, Germany, 2007.
- 39 S. J. Clark, M. D. Segall, C. J. Pickard, P. J. Hasnip, M. J. Probert, K. Refson and M. C. Payne, *Z. Kristallogr.*, 2005, **220**, 567–570.
- 40 J. P. Perdew, K. Burke and M. Ernzerhof, *Phys. Rev. Lett.*, 1996, **77**, 3865–3868.